Available online at www.sciencedirect.com
SCIENCE DIRECT
Polymer 46 (2005) 10017–10026
polymer
www.elsevier.com/locate/polymer

A new biodegradable blends prepared from polylactide and hyaluronic acid

Chin-San Wu*, Hsin-Tzu Liao

Institute of Environmental Polymer Materials, Kao Yuan Institute of Technology, Kaohsiung County, Taiwan 82101, ROC

Received 27 May 2005; accepted 19 August 2005
Available online 8 September 2005

Abstract

In this article, the biodegradable polylactide/hyaluronic acid (PLA/HA) composites were prepared by a melt blending method. In addition, the acrylic acid grafted polylactide (PLA-*g*-AA) was studied as an alternative to PLA. The samples were characterized by a fourier transform infrared (FTIR) spectroscopy, a nuclear magnetic resonance (NMR), a differential scanning calorimetry (DSC), an Instron mechanical tester, and a scanning electron microscopy (SEM). As the result, due to the poor compatibility between PLA and HA, the mechanical properties of PLA/HA composites were worse than PLA. Much better dispersion and homogeneity of HA in the polymer matrix could be obtained when PLA-*g*-AA was used in place of PLA in the composite. The PLA-*g*-AA/HA composites could obviously improve the mechanical properties of PLA/HA ones, and the former provided a plateau tensile strength at break when the HA content was up to 20 wt%. Furthermore, the PLA-*g*-AA/HA was more easily processed than the PLA/HA because the former had lower viscosity than the latter, as they were molten. Biodegradation tests of blends were also studied under the enzymatic environment, and the result showed that the mass of blends reduced by about the HA content within 4 weeks.

Keywords: Polylactide; Hyaluronic acid; Blend

1. Introduction

The use of non-renewable petroleum-based chemicals for the synthesis and manufacture of commercial polymers has caused many environmental problems associated with their disposal. The main strategies to address these problems are to utilize polymeric materials from renewable sources such as starch, cellulose and wood flour, and to develop biodegradable polymeric materials such as polylactic acid (PLA), poly(ε-caprolactone) (PCL) and poly(3-hydroxybutyrate) (PHB).

Polylactic acid (PLA), which can be produced by ring-opening polymerization of lactides and the lactic acid monomers used are obtained from the fermentation of sugar feed stocks, is a degradable thermoplastic polymer with excellent mechanical properties [1–4]. PLA has been found to degrade within a few weeks in soil environments [5]. However, PLA is not widely used because of its high cost as compared to synthetic plastics. To reduce cost, some articles have been proposed to study the composites of PLA and starch and the result shows that the blends have rather poor mechanical properties due to poor adhesion of starch and PLA [5–8]. Varying types of chemicals, such as citrate esters, have been tried to plasticize PLA [9]. Recently, plasticizers such as poly(ethylene glycol) (PEG), glucose monoesters and partial fatty acid esters [10] were used to improve the flexibility and impact resistance of PLA.

The hyaluronic acid (HA), a linear polysaccharide composed of repeating units of *N*-acetyl-glucosamine and D-glucuronic acid, is a component of extracellular matrix (ECM) and it has the high capacity of lubrication, water-sorption and water retention [11,12]. Recently, HA has been widely used in biomedical applications such as scaffolds for wound healing and tissue engineering, ophthalmic surgery, arthritis treatment, and utilization as a component in implant materials [13,14]. Blending of PLA with biodegradable polymers, such as poly(ε-caprolactone) [15], poly(butylenes succinate) [16] and poly(hydroxy butyrate) [17], to produce fully degradable hybrids had been studied but there were no articles about the investigation of PLA/HA blends.

* Corresponding author.
E-mail address: cws1222@cc.kyu.edu.tw (C.-S. Wu).

0032-3861/$ - see front matter © 2005 Elsevier Ltd. All rights reserved.
doi:10.1016/j.polymer.2005.08.056

In this paper, we will systematically investigate the effect of replacing pure PLA with acrylic acid grafted PLA (PLA-*g*-AA) on the structure and properties of PLA/HA composites. The fourier transform infrared (FTIR) spectroscopy and the nuclear magnetic resonance (NMR) are used to characterize the composites, whilst the XRD spectroscopy and the differential scanning calorimetry (DSC) are applied to understand the structural change that occurs with the acrylic acid graft. Meanwhile, a scanning electron microscopy (SEM) and an Instron mechanical tester are used to examine morphology and mechanical properties of the blends. Furthermore, water absorption of synthesized blends and weight loss of blends exposed to enzymatic environment were estimated to assess water resistance and biodegradability.

2. Experimental

2.1. Materials

Polylactide, consisting of 95% L-lactide and 5% *meso*-lactide, was supplied by Cargill-Dow. Acrylic acid (AA) and benzoyl peroxide (BPO) were obtained from Aldrich Chemical Corp. (Milwaukee, WI). Before use, AA was purified by re-crystallization from chloroform and BPO, used as an initiator, was purified by dissolving it in chloroform and reprecipitating with methanol. Hyaluronic acid ($M_W = 1.7 \times 10^6$) was obtained from the Koch-Light Laboratories Ltd. The PLA-*g*-AA copolymer was prepared in our laboratory as described below.

2.2. Grafting reaction of AA onto PLA

A mixture of AA and BPO was added in four equal portions at 2-min intervals to the molten PLA to allow grafting reaction to take place. The reactions were carried out at 85 ± 2 °C under a nitrogen atmosphere at a flow rate of 25 cm^3/min. Preliminary experiments showed that reaction equilibrium was attained in less than 6 h, and reactions were, therefore, allowed to progress for 6 h, at a rotor speed of 60 rpm. The product (4 g) was dissolved in 200 mL of refluxing xylene at 85 °C and the solution was then filtered through several layers of cheesecloth. The xylene-insoluble product remaining on the cheesecloth was washed using acetone to remove the unreacted acrylic acid, and was then dried in a vacuum oven at 80 °C for 24 h. The xylene-soluble product in the filtrate was extracted five times, using 600 mL of cold acetone for each extraction. Using a titration method [18], the grafting percentage was determined as being about 5.95 wt% when BPO loading and AA loading were kept at 0.3 and 10 wt%, respectively.

2.3. Determination of grafting percentage

The acrylic acid loading of the xylene-soluble polymer was calculated from the acid number and the result was expressed as the grafting percentage. About 2 g of copolymer was heated for 2 h in 200 mL of refluxing xylene. This solution was then titrated immediately with a 0.03 N ethanolic KOH solution, which had been standardized against a solution of potassium hydrogen phthalate, whilst phenolphthalein was used as an indicator. The acid number and the grafting percentage could then be calculated using the following equations [18]:

$$\text{Acid number (mgKOH/g)} = \frac{V_{\text{KOH}}(\text{mL}) \times C_{\text{KOH}}(\text{N}) \times 56.1}{\text{polymer(g)}} \quad (1)$$

$$\text{Grafting percentage (\%)} = \frac{\text{Acid number} \times 72}{2 \times 561} \times 100\% \quad (2)$$

2.4. Blends preparation

The blends were prepared by using a Brabender 'Platograph' 200 Nm mixer W50EHT instrument with a blade-type rotor (Duisburg, Germany) under the conditions that the rotor speed, the reaction time and the blending temperature were maintained at 50 rpm, 15 min and 140–150 °C, respectively. The HA was dried in an oven at 105 °C for 24 h prior to blending. For the preparation of blends, mass ratios of HA to PLA (or PLA-*g*-AA) were fixed at 5/95, 10/90, 15/85, and 20/80. After blending, the composites were pressed into thin plates by a hot press at 200 °C and then put into a dryer for cooling. The relative humidity of dryer was set at $50 \pm 5\%$ and the samples were conditioned for 24 h. It has been found that 24 h conditioning time is enough for dehydrating samples to appropriate water content, and that longer storage time does not show appreciable effect on the property of composites.

2.5. NMR/FTIR/DSC analyses

The ^{13}C solid-state NMR spectra were performed via a Bruker AMX 400 ^{13}C NMR spectrometer under the conditions of 50 MHz, cross-polarization, magic anodic angle sample spinning, power decoupling, 90° pulse and 4 s cycle time. Infrared spectra of samples were obtained using a Bio-Rad FTS-7PC type FTIR spectrophotometer. The melting temperature (T_m) and the melting enthalpy (ΔH_m) were determined using a TA instrument 2010 DSC system. For the DSC tests, sample sizes ranged from 4 to 6 mg and the melting curves were recorded from 0 to +250 °C scanned at a heating rate of 10 °C/min.

2.6. Mechanical properties

Following the ASTM D638 method, an Instron mechanical tester (Model Lloyd, LR5K type) was used to measure the tensile strength at breakpoint. By using thin plates (about

1 mm) of the previous conditioned samples, the measurements were conducted at a 20 mm/min crosshead speed. Five measurements were taken for each sample and the data were averaged to obtain a mean value.

2.7. Blend morphology

A scanning electron microscope (Hitachi Microscopy Model S-1400, Japan) was used to study the morphology of blends. Films from the mechanical analysis were treated with hot water at 80 °C for 24 h, thereafter coated with gold and observed using SEM.

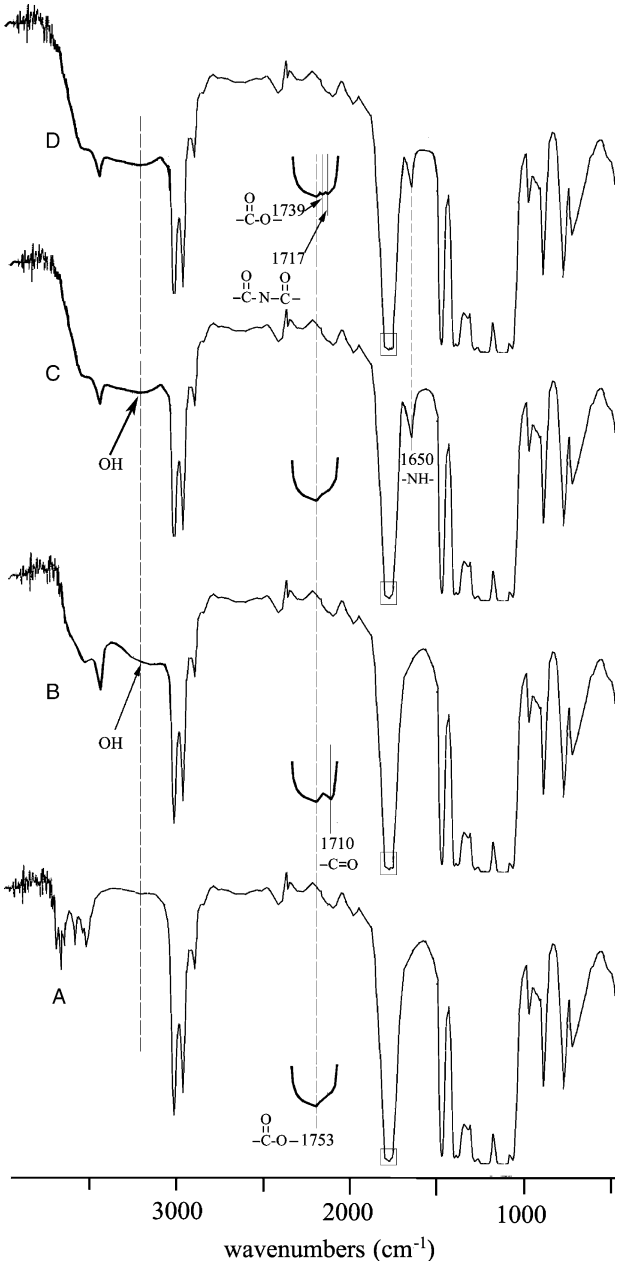

Fig. 1. FTIR spectra of (A) PLA, (B) PLA-*g*-AA, (C) PLA/HA (10 wt%) and (D) PLA-*g*-AA/HA (10 wt%).

2.8. Water absorption

Samples for measuring water absorption were in the form of 75×25 mm strips (150±5 μm thickness) and the testing procedures followed the ASTM D570-81 method. The samples were dried in a vacuum oven at 50±2 °C for 8 h, cooled in a desiccator for 24 h and then immediately weighed to the nearest 0.001 g (designated as W_c). Thereafter, the conditioned samples were immersed in the distilled water, maintained at 25±2 °C, for the 6-week test period. During this period, they were removed from the water at each 1-week interval, gently blotted with tissue paper to remove excess water on the surface, immediately weighed to the nearest 0.001 g (designated as W_w), and returned to the water. Each value of W_w was an average value obtained from three measurements. The final water uptake (designated as $\%W_f$) was calculated to the nearest 0.01% as follows:

$$\%W_f = \frac{W_w - W_c}{W_c} \times 100\%.$$

2.9. Biodegradation studies

Samples were cast into films using a 50×50 mm plastic mold and the resulting films were 0.05±0.02 mm thickness. The films were then washed several times with a large amount of distilled water until the rinsed water was neutral. Afterwards, the film was placed on a piece of glass with the film edges clamped, and then dried in a vacuum oven (50± 2 °C, 0.5 mmHg, and 24 h). Films were then placed in compost petri dishes containing 30 mL phosphate buffer solution (100 mM; pH=6.3) with *p*-cresol (1.8 mM) and

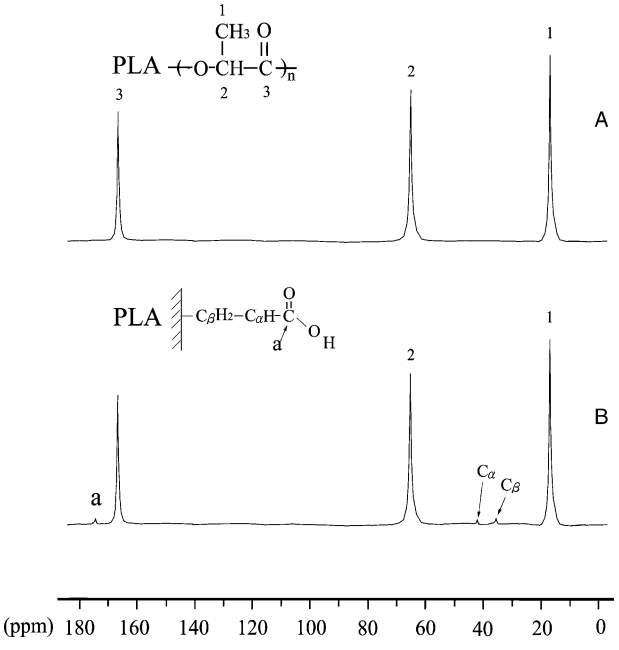

Fig. 2. ^{13}C NMR spectra of PLA and PLA-*g*-AA.

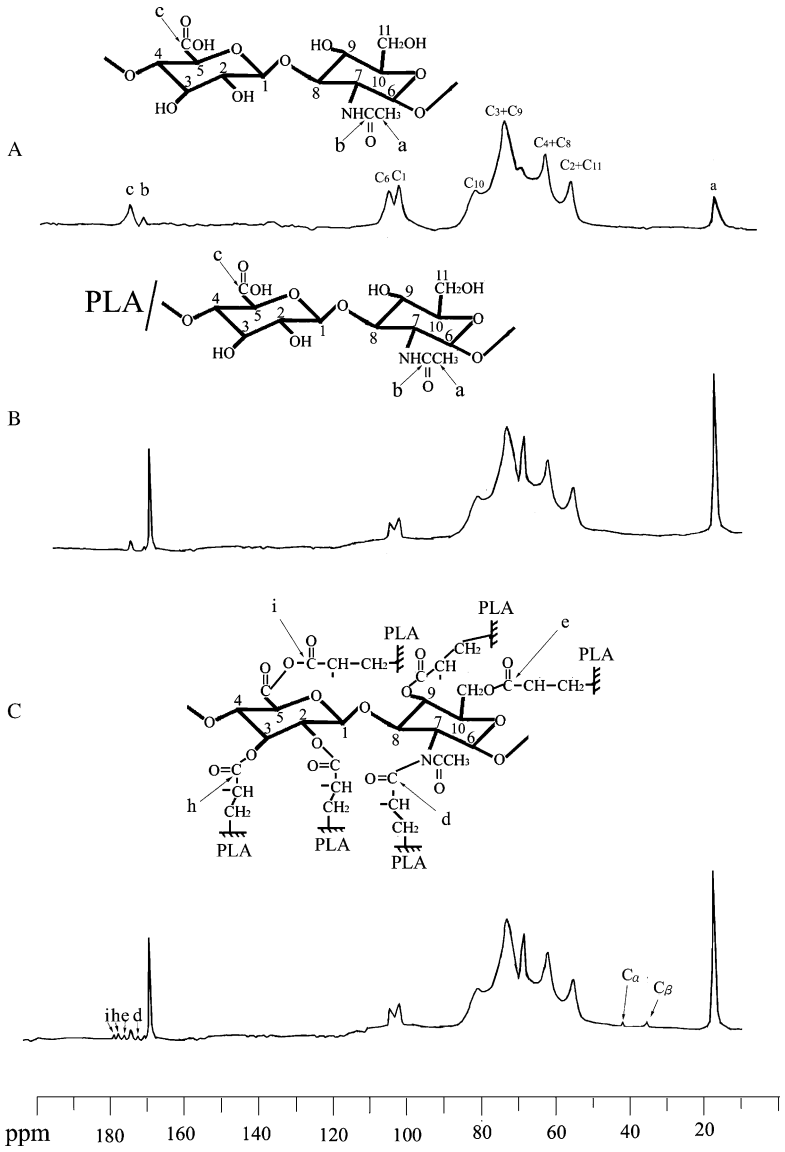

Fig. 3. ^{13}C NMR spectra of (A) HA, (B) PLA/HA (10 wt%) and (C) PLA-*g*-AA/HA (10 wt%).

tyrosinase (20 U/mL), incubated at 35±2 °C and 50±5% relative humidity. After reaction, the films were washed extensively with deionized water and then dried. In this work, the studies were conducted using three replicate test reactors and three replicate samples in each test reactor for each exposure time, meaning that each result was based on nine samples.

3. Results and discussion

3.1. Characterization of PLA-g-AA/HA

FTIR spectroscopy was used to investigate the grafting of acrylic acid onto PLA. The FTIR spectra of PLA and PLA-*g*-AA are shown in Fig. 1(A) and (B). It can be seen that all the characteristic peaks of PLA at 3300–3700, 1700–1760 and 500–1500 cm^{-1} appeared in both polymers [19], but an extra peak was observed for the modified PLA at 1710 cm^{-1}, assigned to –C=O, as well as a broad O–H stretching absorbance at 3200–3700 cm^{-1}. This pattern of peaks demonstrated that acrylic acid had been grafted onto PLA because the discernible shoulder near 1710 cm^{-1} revealed the formation of free acid in the modified polymer. Furthermore, Fig. 1(C) and (D) gave the FTIR spectra of PLA/HA(10 wt%) and PLA-*g*-AA/HA(10 wt%). A comparison between spectra of PLA/HA(10 wt%) and PLA showed that the peak assigned to O–H bond stretching vibration at 3200–3700 cm^{-1} was much more intense for PLA/HA(10 wt%) blend. This is due to the –OH group of hyaluronic acid, which attributes to the bond stretching vibration [20,21]. In addition, with comparison between the FTIR spectra of PLA/HA (10 wt%) and PLA-*g*-AA/HA (10 wt%), a new absorption peak at 1739 cm^{-1} in Fig. 1(D)

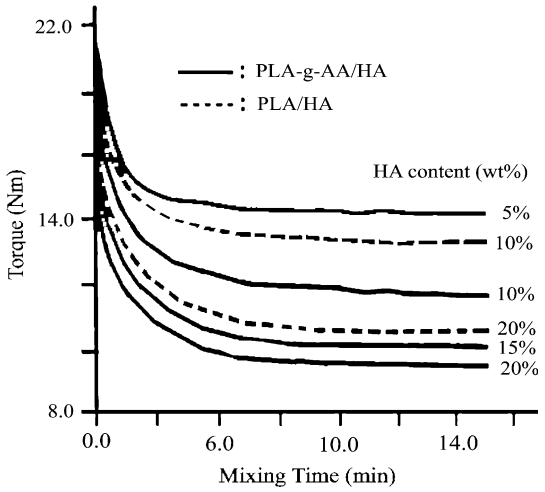

Fig. 4. Torque value vs. mixing time for preparation of PLA/HA and PLA-*g*-AA/HA blends at various HA contents.

could be observed, which was assigned to the ester carbonyl stretching vibration in copolymer. Expansion of FTIR spectra in the limited range of 1700–1760 cm^{-1} in Fig. 1 more clearly shows the difference between spectra of PLA/HA and PLA-*g*-AA/HA. As shown in Fig. 1(A), for the PLA, the –C=O stretching vibration appeared as a strong broad band at 1700–1760 cm^{-1}. As the spectrum of the PLA/HA(10 wt%) blend (Fig. 1(C)), –C=O stretching vibration still leaded to broad absorption band at 1750–1760 cm^{-1}, while the spectra of PLA-*g*-AA/HA (Fig. 1(D)) exhibited that two extra peaks were newly formed at 1739 cm^{-1}. This result is supported by the study of Wu et al. [22] in which the FTIR spectrum of ester carbonyl showed its absorption peak at 1739 cm^{-1}. Based on the above result, one can infer that branched and cross-linked macromolecules may be produced in PLA-*g*-AA/HA because the copolymer has carboxyl groups to react with the hydroxyl groups of HA. The peak at 1717 cm^{-1} is assigned to –C=O of $N(COR)_2$ while the peak at 1739 cm^{-1} is due to the absorption of –C=O in OCOR. These ester and imide functional groups are formed via the reaction between –OH of PLA-*g*-AA and –NH of hyaluronic acid when the two polymers are blended. Additionally, the appearance of peak at spectra 1650 cm^{-1} in Fig. 1(C) and (D) revealed the formation of primary amide in both PLA/HA and PLA-*g*-AA/HA blends. This result, similar to that obtained by Alkrad et al. [23], indicated that in the blending of PLA-*g*-AA with hyaluronic acid, part of the primary amide of hyaluronic acid has reacted with the carboxyl group of PLA-*g*-AA.

To further confirm the grafting of AA onto PLA, ^{13}C NMR was used to compare the structure of PLA and PLA-*g*-AA, and the result was shown in Fig. 2. Carbon peaks occurred in three places for unmodified PLA (1: $\delta=$ 16.91 ppm, 2: $\delta=68.76$ ppm, and 3: $\delta=169.96$ ppm). A similar result had been reported by Breitenbach et al. [24], in which lactic acid and glycolic acid copolyester was studied. A comparison between the ^{13}C NMR spectra of PLA and PLA-*g*-AA showed that the latter had three extra peaks (C_β: $\delta=35.61$ ppm; C_α: $\delta=42.21$ ppm; *a*: $\delta=$ 175.03 ppm). These extra peaks, C_α, C_β and '*a*', confirmed that AA had been indeed grafted onto PLA, and the corresponding structure is illustrated in Fig. 2(B) [25].

The solid-state ^{13}C NMR spectra of original hyaluronic acid, PLA/HA (10 wt%), and PLA-*g*-AA/HA (10 wt%) were shown in Fig. 3. The spectrum of original hyaluronic acid was the same as that reported by Alkrad et al. [23] Comparing signals between the spectra of PLA/HA (10 wt%) and PLA-*g*-AA/HA (10 wt%), we found that there were extra peaks at $\delta=42.19$ ppm (C_α) and $\delta=$ 35.63 ppm (C_β) in the latter. As already indicated, the appearance of peaks at C_α and C_β in PLA-*g*-AA was due to grafting of AA onto PLA. However, the peak at $\delta=$ 175.05 ppm (C=O) (shown in Fig. 2(B)) was absent in the solid state spectrum of PLA-*g*-AA/HA (10 wt%) (Fig. 3(C))

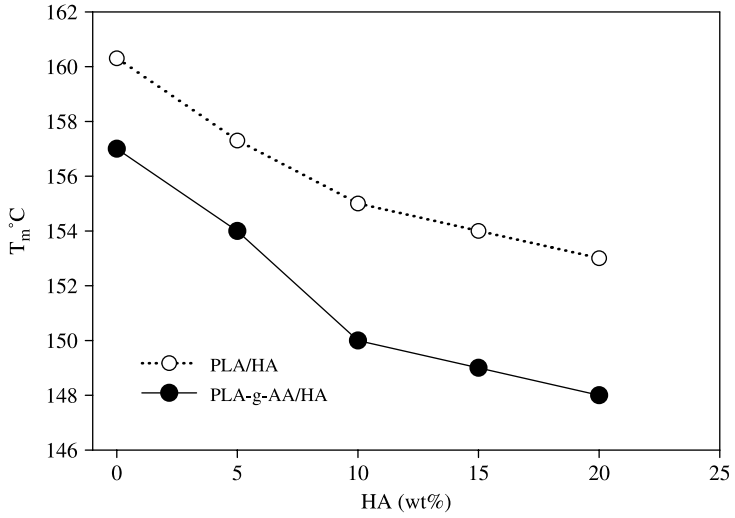

Fig. 5. Melting temperature vs. HA content for PLA/HA and PLA-*g*-AA/HA blends.

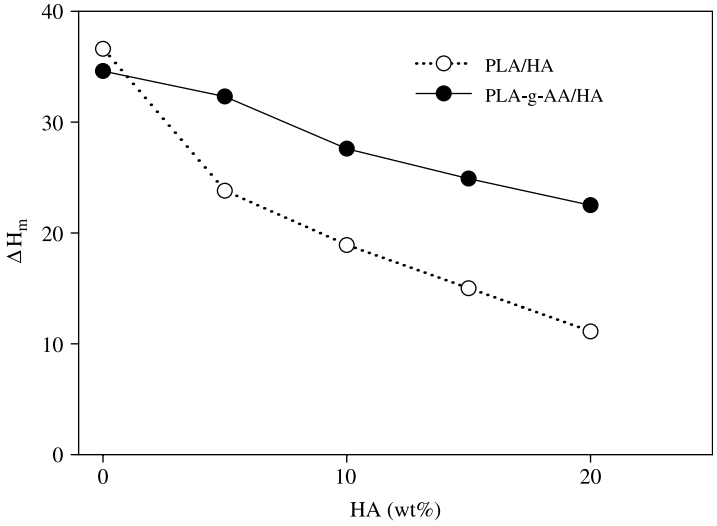

Fig. 6. Melting enthalpy vs. HA content for PLA/HA and PLA-*g*-AA/HA blends.

but it shifted to the duplicates at i, e, h, and d ($\delta = 178.9$, 177.7, 173.9 and 171.2 ppm). The peaks at i, e, h, and d gave the evidence of the condensation reaction between –COOH of PLA-*g*-AA and –OH or –NH of HA. Via this condensation reaction, the original HA was fully acylated, and amide groups were converted to imides (represented by peaks d, e and f in Fig. 3(C)). This reaction did not occur between PLA and HA, as illustrated by the absence of corresponding peaks in the PLA/HA (10 wt%) spectrum (Fig. 3(B)). Formation of imide and ester functional groups noticeably affected the thermal, mechanical and biodegradation properties of PLA-*g*-AA/HA, which will be discussed in the following sections.

3.2. Torque measurements

The variation of torque with blending time for PLA/HA and PLA-*g*-AA/HA blends was presented in Fig. 4. The torque value of both blends decreased with increasing HA content and blending time, and approached a stable value when the blending time was greater than 8 min, suggesting that good mixing had occurred after about 10 min. Final torque decreased with increasing HA content because the viscosity of molten HA was lower than that of molten PLA or PLA-*g*-AA. Further, the torque response of PLA-*g*-AA/HA was significantly lower than that of PLA/HA at the same HA content (10 and 20 wt%). The improved rheological behavior of PLA-*g*-AA/HA was attributed to the conformational change of the hyaluronic acid molecule [26], caused by the formation of an ester functional group as previous discussion.

Table 1
The hyaluronic acid phase size of PLA/HA and PLA-*g*-AA/HA blends at different hyaluronic acid contents

HA (wt%)	Phase size (μm)	
	PLA/HA	PLA-*g*-AA/HA
5	53	28
10	65	32
15	73	34
20	82	36

3.3. Differential scanning calorimetry analysis

The differential scanning calorimetry was used to study the thermal properties of blends. Figs. 5 and 6 gave the melting temperature (T_m) and the melting enthalpy (ΔH_m), determined from the DSC heating thermograms but not shown here, of PLA/HA and PLA-*g*-AA/HA blends at different hyaluronic acid contents. For both blends, a decrease in melting temperature was observed with increasing hyaluronic acid content (Fig. 5). This is due to the lower melt viscosity of hyaluronic acid, as discussed previously. With the same hyaluronic acid content, the PLA/HA blend had a higher melting temperature than the PLA-*g*-AA/HA blend. This result was in accordance with the corresponding torque measurements, which showed that PLA-*g*-AA/HA blends had a lower melt torque than PLA/HA blends at the same hyaluronic acid content. These phenomena (lower values of melting temperature and torque) also accorded with the lower melting viscosity of PLA-*g*-AA/HA. This lower melting viscosity means that PLA-*g*-AA/HA is more easily processed than PLA/HA.

The melting enthalpy (ΔH_m) of pure PLA was 36.5 J/g, whilst that of PLA-*g*-AA was 34.3 J/g (Fig. 6). The lower melting enthalpy of PLA-*g*-AA is probably due to grafted branches that disrupt the regularity of the chain structures in PLA and increase the spacing between the chains [27]. With the same hyaluronic acid content, however, the AA grafted composites (PLA-*g*-AA/HA) produced higher ΔH_m value (about 8–15 J/g) than the PLA/HA ones. This higher ΔH_m is due to the ester carbonyl functional group generated from the reaction between the –OH groups of HA and the –COOH groups of PLA-*g*-AA.

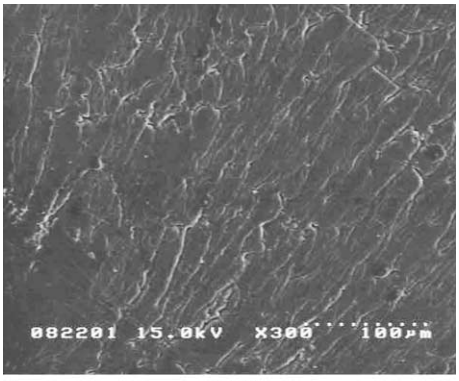

A PLA

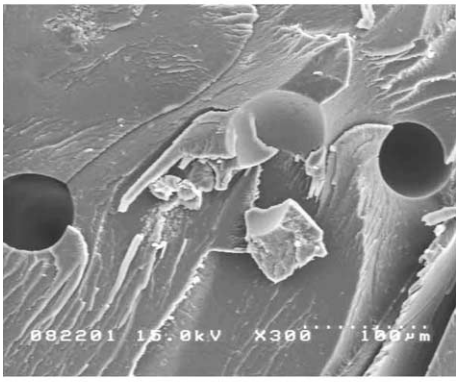

B PLA/HA (10wt%)

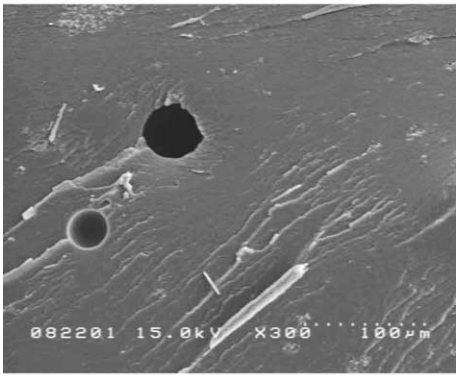

C PLA-g-AA/HA(10wt%)

Fig. 7. SEM micrographs of PLA and its blends.

The ΔH_m can be used as an indication of percentage crystallinity of the blend. Fig. 6 showed that the ΔH_m of both blends clearly decreased as the HA content increased. The decrease in ΔH_m, and therefore, crystallinity, of PLA/HA was much more marked. These findings were similar to those of Wu [28], who studied the properties of chitosan and polyethylene–octene elastomer blends. The marked decrease in crystallinity of PLA/HA is probably due to the result of the hyaluronic acid prohibiting the movement of the polymer segments, causing polymer chain arrangement to become more difficult, and also because the hydrophilic character of hyaluronic acid leads to poor adhesion with the hydrophobic PLA [4,29], causing a steric effect.

3.4. Composite morphology

It is necessary to study the morphology of the polymer blends since their mechanical properties depend on it. In the PLA/HA and PLA-*g*-AA/HA blends, the major component (PLA or PLA-*g*-AA) forms the matrix whereas the minor component (hyaluronic acid) is the dispersed phase. SEM micrographs of pure PLA, PLA/HA, and PLA-*g*-AA/HA were presented in Fig. 7. From the morphology of PLA/HA blend containing 10 wt% hyaluronic acid, Fig. 7(B), it can be found that the average pore diameter of its fracture surface is about 65 μm. Thus, by examining the morphology of the blends having different HA contents (not shown here), the variation of average pore diameter with HA contents for PLA/HA and PLA-*g*-AA/HA was illustrated in Table 1. For both blends, it can be seen that the size of the HA phase increases with an increasing content of hyaluronic acid. It is remarkable that there is a fine dispersion and homogeneity of hyaluronic acid in the PLA matrix for PLA/HA blends, as the hyaluronic acid content is less than 10 wt%. The large sizes of hyaluronic acid phases produced, especially in the blend containing 20 wt% hyaluronic acid, suggest that the adhesion between hyaluronic acid and PLA is very poor and that the two polymers are strongly incompatible [30].

When the PLA-*g*-AA copolymer is used to replace the PLA, Fig. 7(C) and Table 1, the size of hyaluronic acid phase decreases compared to the corresponding PLA/HA blends. Table 1 also shows there is a fine dispersion and homogeneity of HA in the PLA-*g*-AA matrix for hyaluronic acid content up to 20 wt%. The phase size in all PLA-*g*-AA/HA blends is lower than 36 μm and is detectable only in higher magnification; and this better dispersion arises from the formation of branched and crosslinked macromolecules since this PLA-*g*-AA copolymer has anhydride groups to react with the hydroxyls of hyaluronic acid. The result is a reduction in the interfacial tension between the two polymers and a finer distribution of HA in all PLA-*g*-AA/HA blends.

3.5. Mechanical properties

Fig. 8 showed the effect of hyaluronic acid content on the tensile strength at breakpoint for PLA/HA and PLA-*g*-AA/HA composites. For PLA/HA composites, the tensile strength at breakpoint decreased continuously and markedly as HA content increased. The composite containing 20 wt% hyaluronic acid gave the lowest tensile strength at breakpoint because the higher hyaluronic acid content increased the phase size. It is thus clear that mechanical incompatibility of the two polymers is great. For PLA-*g*-AA/HA composites, the tensile strength at breakpoint decreased slightly as HA content increased though the tensile strength of PLA-*g*-AA is smaller than that of pure PLA. The absolute value of tensile strength at breakpoint for all PLA-*g*-AA/HA composites was, indeed, evidently higher than that of PLA/HA ones. It was also found that the PLA-*g*-AA composites provided a plateau tensile strength at break when the HA

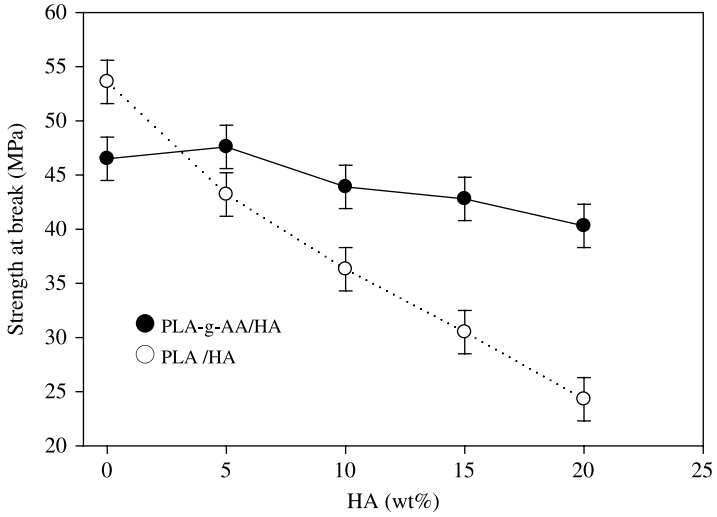

Fig. 8. Tensile strength at breakpoint vs. HA content for PLA-*g*-AA/HA and PLA/HA blends.

content was up to 20 wt%. It is evident that the mechanical properties strongly depend on the dispersion and phase size of HA in the polymer matrix. With a smaller dispersed phase, an increase in mechanical properties, especially in tensile strength, was observed for PLA-*g*-AA/HA composites.

3.6. Water absorption

Fig. 9 illustrated the variation of water uptake gain with time during water absorption period for PLA, PLA-*g*-AA, PLA/HA, and PLA-*g*-AA/HA. It can be seen that the water resistance of PLA was somewhat better than that of PLA-*g*-AA but the PLA-*g*-AA/HA blend exhibited better water resistance than the PLA/HA blend at the same hyaluronic acid content. The lower water absorption of PLA-*g*-AA/HA, as compared with PLA/HA, was attributed to the formation of ester carbonyl functional groups. For both blends, the water uptake gain over the 6-week test period increased with hyaluronic acid content. This was probably due to the increased difficulty in forming polymer chain arrangements with greater amounts of HA, and to the hydrophilic character of hyaluronic acid causing poor adhesion with the hydrophobic PLA.

3.7. Biodegradation analysis

In general, carbon dioxide, water and other harmless materials are produced via the fungus biodegradation of biopolymers and their mechanical nature will have apparent changes. In this study, the test focused on the PLA and its blends, and the results were given in Figs. 10–12. Fig. 10 showed the changes in weight loss with exposed time for PLA/HA and PLA-*g*-AA/HA blends, having HA contents of 0, 10, and 20 wt%, through the enzymatic biodegradation process. During the period of biodegradation test, the water diffused into the polymer sample, causing swelling and enhancing biodegradation. The blends containing a higher

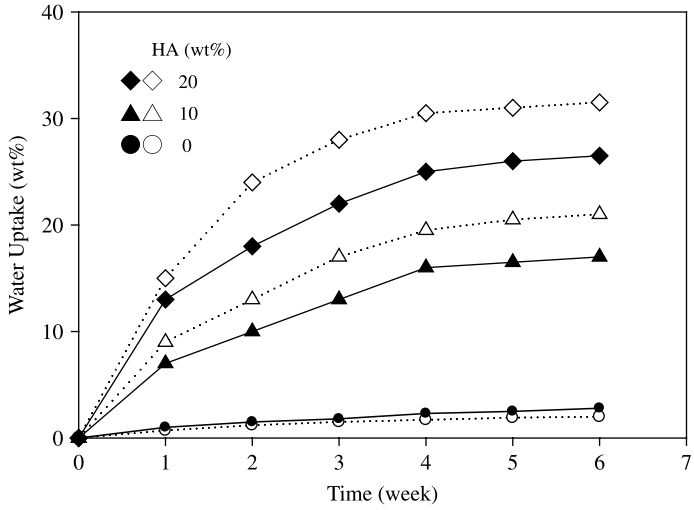

Fig. 9. Water uptake of blends during water absorption (the dotted and solid lines indicate PLA/HA and PLA-*g*-AA/HA, respectively).

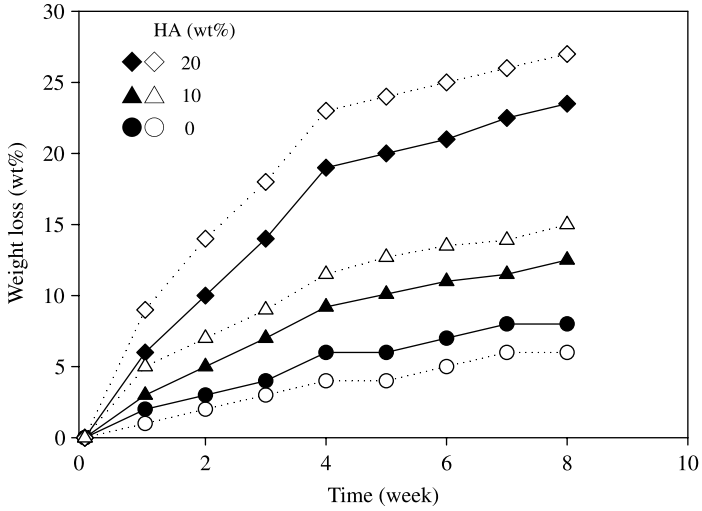

Fig. 10. Weight loss of blends exposed to the enzymatic environment (The dotted and solid lines indicate PLA/HA and PLA-*g*-AA/HA, respectively).

percentage of hyaluronic acid (20 wt%) degraded rapidly in the initial 4 weeks, equivalent to the approximate hyaluronic acid content of the blends, and a gradual decrease of weight occurred during the next 4 weeks. The weight loss of both blends, which indicated the extent of biodegradation of the blends, increased as the content of hyaluronic acid increased. Further comparison of the two blends revealed that PLA/HA had a higher value of weight loss, with an increment of about 2–5 wt%. The greater biodegradation of PLA/HA may be caused by the factor that there were poor adhesion and dispersivity between PLA and HA.

To further study the change of structure of PLA/HA blend and pure PLA after biodegradation test. Figs. 11 and 12 showed the micrographs of pure PLA and PLA/HA blend exposed to the enzymatic environment, respectively. As expected, the destruction of blend surface was severer while the time exposed to the enzymatic environment was increased. It was found from Fig. 11 that the surface of pure PLA was smooth before biodegradation test but, after 5-week test, some fungi grew on the polymer surface and then the polymer surface was corrupted and formed micro-holes, observed as white beads of Fig. 11(B). So, the efficiency of biodegradation of PLA under the enzymatic environment (tyrosinase) is not good.

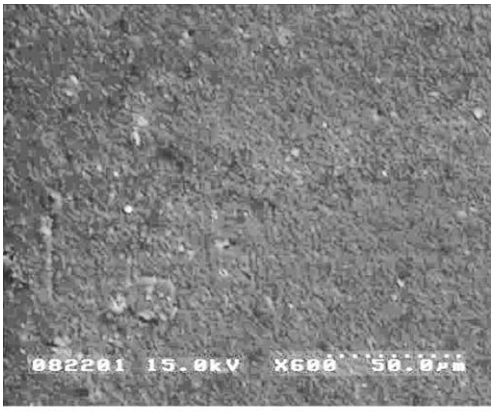

A 0 week

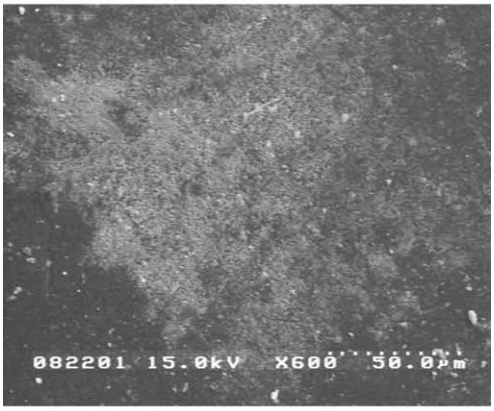

B 5 weeks

Fig. 11. SEM micrographs of pure PLA exposed to the enzymatic environment.

Fig. 12 illustrated SEM microphotographs of PLA/HA (10 wt%) blend after 0, 1, 2, 4, 6 and 8-week biodegradation tests. It could be seen that the surface of PLA/HA was cracked slowly in the enzymatic environment during the first week but the fungi produced little holes on the polymer surface via the decomposition of HA after 2 weeks. After 4 weeks, the fungi corrupted the polymer surface and formed bigger round holes; this was the phenomenon produced by the action of fungi on the biodegradable material (HA). After 8 weeks, the break of the entire round holes indicated that the HA part of the copolymer was nearly completely decomposed by the fungi. This result can be supported by the weight loss of blends presented in Fig. 10.

4. Conclusions

By using PLA-*g*-AA to replace PLA for preparation of blends, the mechanical properties of a PLA/HA-type

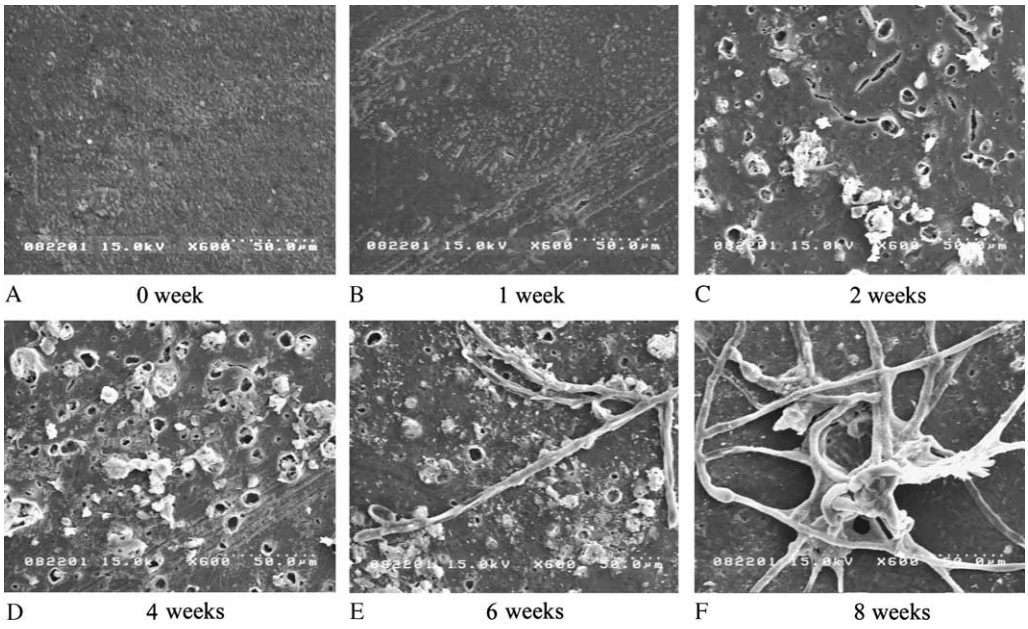

Fig. 12. SEM micrographs of PLA/HA (10 wt%) exposed to the enzymatic environment.

composite can be improved. The crystalline structure of PLA-*g*-AA/HA differs from that of PLA/HA, due to the formation of an ester carbonyl functional group from the reaction between the –OH of HA and the –COOH of PLA-*g*-AA. For PLA/HA blends, the melting temperature (T_m) and the melting enthalpy (ΔH_m) both decreased with increasing hyaluronic acid content. When PLA was replaced with PLA-*g*-AA, the PLA-*g*-AA/HA gave higher T_m and lower ΔH_m than those of PLA/HA. Morphology of PLA/HA blends indicated that the hyaluronic acid phase size increased with increasing hyaluronic acid content, suggesting that the compatibility between PLA and hyaluronic acid was very poor. For PLA-*g*-AA/HA blends, the size of the hyaluronic acid phase was noticeably reduced and, being always less than 36 μm, was detectable only under higher magnification. Tensile strength at breakpoint of PLA/HA blends decreased markedly and continuously as hyaluronic acid content was increased. The composite containing PLA-*g*-AA exhibits enhanced mechanical properties compared with that containing PLA, especially regarding tensile strength at breakpoint. The water resistance of PLA-*g*-AA/HA was higher than that of PLA/HA. Finally, the effect of enzyme (tyrosinase) on biodegradation of PLA was slight but marked for HA.

References

[1] Tsuji H, Ikada Y. J Appl Polym Sci 1998;67:405–15.
[2] Lunt J. Polym Degrad Stab 1998;59:145–52.
[3] Drumright RE, Gruber PR, Henton DE. Adv Mater 2000;12:1841–6.
[4] Hakkarainen M. Adv Polym Sci 2002;157:113–38.
[5] Shogren RL, Doane WM, Garlotta D, Lawton JW, Willett JL. Polym Degrad Stab 2003;79:405–11.
[6] Kim SH, Chin I, Yoon J, Kim SH, Jung J. Korean Polym J 1998;6:422–7.
[7] Ke T, Sun X. Cereal Chem 2000;77:761–8.
[8] Park YD, Tirelli N, Hubbell JA. Biomaterials 2003;24:893–900.
[9] Martin O, Averous L. Polymer 2001;42:6209–19.
[10] Hoffman AS. Adv Drug Deliv Rev 2002;43:3–12.
[11] Magnani A, Silverstri V, Barbucci R. Macromol Chem Phys 1999;200:2003–14.
[12] Kitano T, Ateshian GA, Mow VC, Kadoya Y, Yamano Y. J Biomech 2001;34:1031–7.
[13] Bakos D, Soldan M, Hernandez-Fuentes I. Biomaterials 1999;20:191–5.
[14] Pavesio A, Renier D, Cassinelli C, Morra M. Med Device Technol 1997;8:24–7.
[15] Wang L, Ma W, Gross RA, McCarthy SP. Polym Degrad Stab 1998;59:161–8.
[16] Ikehara T, Nishikawa Y, Nishi T. Polymer 2003;44:6657–61.
[17] Bendix D. Polym Degrad Stab 1998;59:129–35.
[18] Gaylord NG, Mehta R, Kumar V, Tazi M. J Appl Polym Sci 1989;38:359–71.
[19] Yao F, Chen W, Wang H, Lin H, Yao K, Sun P, et al. Polymer 2003;44:6435–41.
[20] Cho KY, Chung TW, Kim BC, Kim MK, Lee JH, Wee WR, et al. Int J Pharm 2003;260:83–91.
[21] Mason M, Vercruysse KP, Kirker KR, Frisch R, Marecak DM, Prestwich GD, et al. Biomaterials 2000;21:31–6.
[22] Wu CS. Polym Degrad Stab 2003;80:127–34.
[23] Alkrad JA, Mrestani Y, Stroehl D, Wartewig S, Neubert R. J Pharm Biomed Anal 2003;31:545–50.
[24] Breitenbach A, Li YX, Kissel T. J Controlled Release 2000;64:167–78.
[25] Wu CS, Liao SM, Laio HT. J Appl Polym Sci 2002;85:2905–12.
[26] Liao H-T, Wu CS. J Appl Polym Sci 2003;88:1919–24.
[27] Willett JL, Shogern RL. Polymer 2002;43:5935–47.
[28] Wu CS. J Polym Sci, Part A: Polym Chem 2003;41:3882–91.
[29] Wu CS. J Appl Polym Sci 2003;89:2888–95.
[30] Bikiaris D, Panayiotou C. J Appl Plym Sci 1998;70:1503–21.